

• Modeling Cellular Effects of Coal Pollutants

Increasing interest in coal and in coal-derived fossil fuels as energy sources has prompted renewed concern over the environmental and health impacts resulting from coal refinement and combustion. The goal of this project is to develop and test models for the dose and dose-rate dependence of biological effects of coal pollutants on mammalian cells in tissue culture. Particular attention is given to the interaction of pollutants with the genetic material (deoxyribonucleic acid, or DNA) in the cell because the work of McCann and Ames (1975) has demonstrated a strong correlation between mutagenesis and cancer induction. Unlike radiation, which can interact directly with chromatin, chemical pollutants undergo numerous changes before the ultimate carcinogen becomes covalently bound to the DNA. Synthetic vesicles formed from a phospholipid bilayer are being used to investigate chemical transformations that may occur during the transport of pollutants across cellular membranes. The initial damage to DNA is rapidly modified by enzymatic repair systems in most living organisms. Increased cancer incidence among humans with hereditary repair deficiencies suggests that repair processes are important in reducing the risk to the normal population from chronic exposure to low levels of carcinogens. A model has been developed for predicting the effects of excision repair (the removal of carcinogen residues from DNA) on the survival of human cells exposed to chemical carcinogens. In addition to the excision system, normal human cells also have tolerance mechanisms that permit continued growth and division of cells without removal of the damage. We are investigating the biological effect of damage passed to daughter cells by these tolerance mechanisms. Chinese hamster ovary cells are being used for these studies because they tolerate a larger degree of carcinogenic damage than human cells. We feel that these cellular studies are a valuable complement to whole-animal and epidemiological studies in assessing the health effects of coal-related pollutants.

Modeling the Dose-Response Relationship for Survival of Human Cells Exposed to Chemical Carcinogens

J. H. Miller

The ability of cells to repair damage to deoxyribonucleic acid (DNA) molecules is an important factor in determining the cytotoxic and mutagenic effect of chemical carcinogens at a given dose. This fact is consistently demonstrated by the differential cytotoxicity between normal human cells and cells from patients with the disease xeroderma pigmentosum (XP). Because of a genetic deficiency, XP cells have a greatly reduced ability to excise some carcinogen adducts from their DNA. An analogous situation exists in the repair of damage induced by ultraviolet (UV) irradiation in the excision-repair-deficient bacteria Escherichia coli Uvr⁻.

For the bacteria case, Haynes (1975) demonstrated that the survival of normal cells after UV irradiation can be predicted if the sensitivity of the repair-deficient mutant and the kinetics of excision in the normal cell are known. We have applied the same type of model to the cytotoxicity induced in normal and XP human fibroblasts by the carcinogen N-acetoxy-2-acetylaminofluorene (N-AcO-AAF). Compounds of this type may result from the in-vivo reduction of nitrate derivatives of benzo[a]pyrene. A paper on this work, which is being done in collaboration with Dr. R. H. Heflich at the National Center for Toxicology Research, has been accepted for publication in the proceedings of the 20th Hanford Life Sciences Symposium.

Little is known about the mechanism of reproductive death in cells exposed to chemical carcinogen. Although bonding to

molecules other than DNA may play a role in the biological response, the data of Heflich et al. (1980) suggest that potentially lethal damage and residues bound to DNA are removed at the same rate. Our model assumes that the mechanism of reproductive death involves an expression time during which potentially lethal damage is removed from the DNA of cells capable of excision repair. This leads to the relationship

$$\ln S = \ln S_{XPA} (1 - f) \quad (1)$$

between the survival S of cells that excise a fraction f of the damage and the survival of XP cells from complementation group A, which do not exhibit any excision of AAF residues.

Figure 1.6 compares the survival of cloning ability in fibroblasts from normal humans with that from XP patients from several complementation groups (Maher et al. 1975; Heflich et al. 1980). Both the concentration of N-AcO-AAF in the growth medium and the initial number of residues bound to DNA are shown on the horizontal axis. From the dose that results in 37% survival of XPA cells, we estimate that about 10^5 residues are required to produce an average of one potentially lethal event per cell. The small probability that a residue will cause reproductive death may be due to nonessential genes in the human chromosome and to repair phenomena other than excision that permit replication of DNA on a damaged template. (The possibility of subsequent biological effects

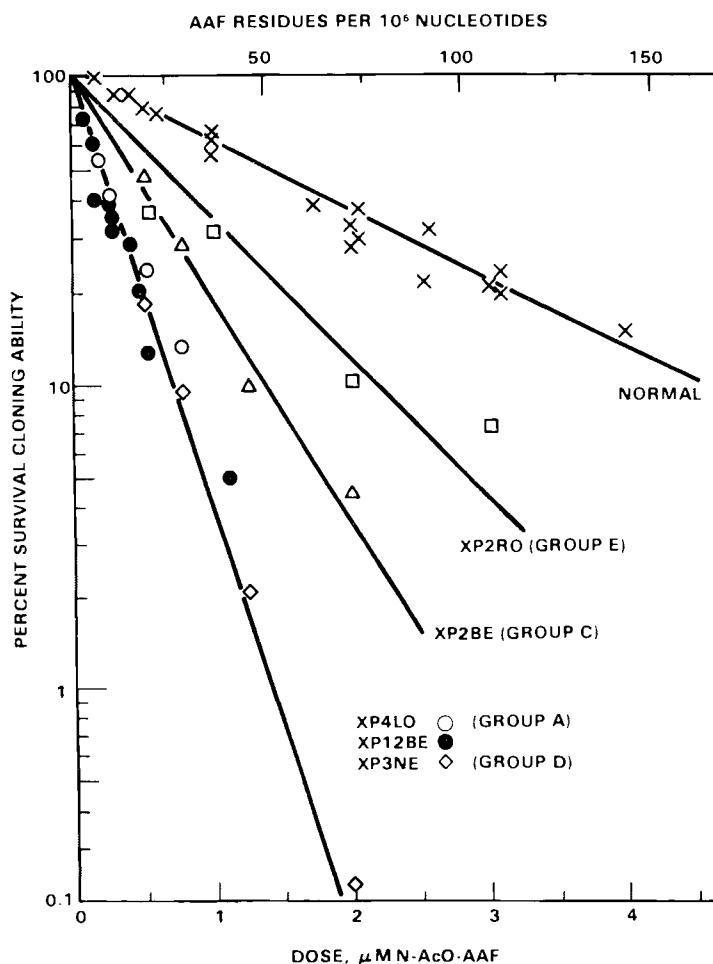


Figure 1.6. Survival of Normal and Xeroderma Pigmentosum (XP) Fibroblasts After Exposure to N-Acetoxy-2-Acetylaminofluorene (N-AcO-AAF)

resulting from damage passed to daughter cells is discussed in the following article in this report.)

The principal objective of our model is to obtain a quantitative correlation between survival data, such as those shown in Figure 1.6, and data derived from biochemical repair studies. If the excision of residues obeys classical enzyme kinetics, then the rate of excision is given by the Michaelis-Menton equation

$$\frac{d[P]}{dt} = \frac{V[R]}{K + [R]} \quad (2)$$

where R is the concentration of carcinogen residues, P is the concentration of excised product, V is the high-dose limit of the removal velocity, and K is the dose at which the rate of removal is half its maximum value. When $[R] \ll K$, Equation 2 reduces to a first-order rate equation, and the number of residues decays exponentially with a lifetime $t = K/V$.

Levinson et al. (1979) have proposed a procession model of excision repair in which the repair enzymes travel unidirectionally along the DNA strand, rather than randomly attaching and detaching as is assumed in the classical model. In the processive model, the rate of excision does not decrease as residues are removed but maintains a constant value that is a function of the initial number of adducts on DNA. If k_t is the rate of travel of the repair complex along the DNA strand and k_e is the rate of excision and resynthesis at the damage site, then the rate of removal

is related to the initial number of bound residues by a Michaelis-Menton equation with $V = k_e E$ and $K = k_e/k_t$.

Figure 1.7 shows the time course for removal of AAF residues at a dose less than 5 μ M. The solid line shows a fit assuming a constant rate of removal over the first 18 h after treatment. The dashed curve illustrates the predictions of the classical first-order model with an initial removal rate equal to that of the processive model. The scatter in the data is too large to allow the two models to be distinguished on the basis of accuracy of fit.

Figure 1.8 shows the initial removal rate as a function of the initial number of bound residues. In most cases, the initial velocity was estimated from measurement of the number of adducts present 18 h after treatment. This procedure slightly underestimates the initial velocity if the number of residues decays exponentially instead of linearly. The data shown in Figure 1.8 cannot be used to distinguish between processive and classical kinetics because both models predict a Michaelis-Menton type of relation for the dose dependence of the initial removal velocity. Hence we conclude that the biochemical repair data currently available are consistent with either model. The data in Figure 1.8 show that if the classical model is valid, then 1) first-order kinetics are a good approximation in the dose range of the survival data shown in Figure 1.6, and 2) the mean lifetime of AAF residues on DNA in the normal human fibroblast is about 70 h.

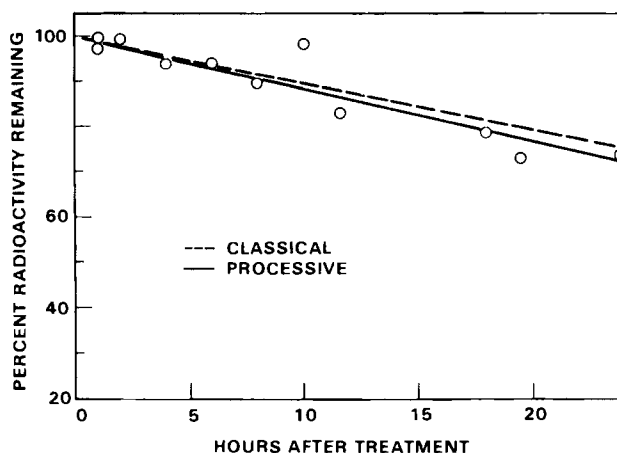


Figure 1.7. Fraction of AAF Residues Bonded to DNA as a Function of Time After Treatment

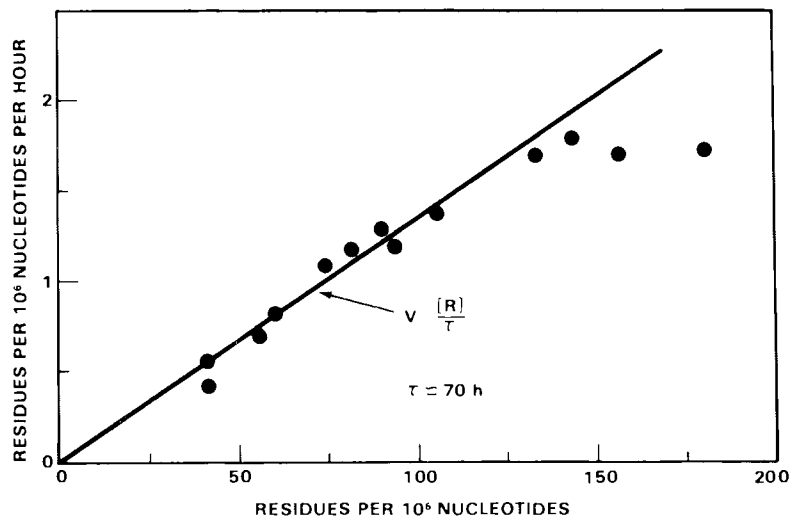


Figure 1.8. Initial Rate of Excision of AAF Residues in Confluent Human Fibroblasts as a Function of Initial Number of Bond Adducts

If the excision of AAF residues obeys classical first-order kinetics, then our model predicts a dose-response relationship of

$$\ln S = \ln S_{XPA} e^{-T/\tau} \quad (3)$$

If the processive model is correct, the survival should be given by

$$\ln S = \ln S_{XPA} (1 - T/\tau) \quad (4)$$

Equations (3) and (4) both predict an exponential survival curve, since the survival response of XP cells from complementation group A is exponential. Excision repair modifies the slope of the plot of $\ln S$ versus dose, making it less negative as a larger fraction of the damage is excised. Hence these simple models cannot account for shoulder effects such as that shown in Figure 1.6 for normal cells.

One way to explain this shoulder is to assume that excision of AAF residues is predominantly a first-order process but has a processive component that saturates at low dose and a maximum velocity that is small compared to the data in Figure 1.8. Other possible explanations for the shoulder on the dose-response curve for normal cells include 1) effects related to the kinetics of bonding and/or nonrandom bonding, 2) biological effects of damage passed to daughter cells by tolerance mechanisms, and 3) interactions between carcinogen residues.

More data at low dose are needed to develop and test models for the shoulder region of the dose-response relationship. We are testing the prediction of Equations (3) and (4) regarding the slope of the exponential part of the survival curve. One experiment in progress concerns the survival of partially repair-deficient XP cells. Figure 1.6 suggests that the fraction of AAF residues excised by XP cells from complementation groups C and E is substantially less than the fraction excised by normal cells. One way to account for this difference is to assume that under the same experimental conditions, all three cell lines have the same time available to excise AAF residues before the damage can be expressed as reproductive death. The difference in the extent of repair is then due to the difference in the rate of excision. If excision is a first-order process, then the ratio of the repair rates in normal, XP2RO, and XP2BE cells would be 1:0.6:0.4. These ratios would be 1:0.8:0.6 for processive repair kinetics. More survival and repair studies are planned with the cells XP2RO and XP2BE to test these predictions.

Figure 1.9 shows the results of another experiment designed to test our model of the dose-response relationship. Normal human cells in a confluent state were treated with N-AcO-AAF and then held at confluence to recover from the damage. They were then replated at low density to score survivors. At a given dose, survival increases with

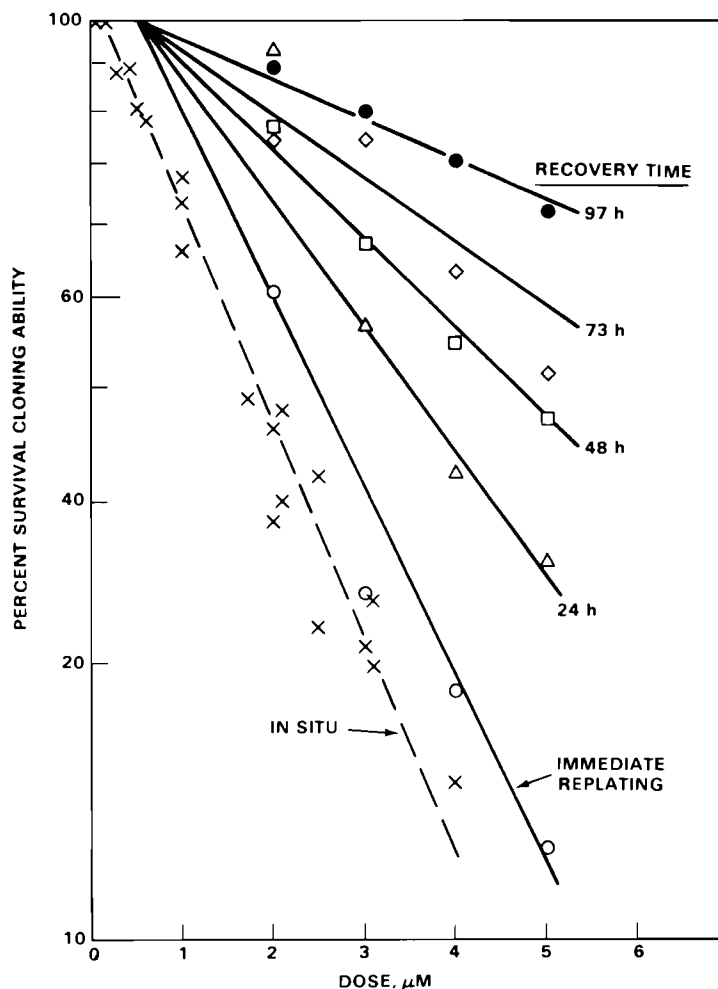


Figure 1.9. Survival of Normal Human Fibroblasts Treated with N-AcO-AAF and Held in a Nonproliferating State Before Replating to Measure Cloning Efficiency

recovery time, as would be expected if the time spent in the nonproliferating state increased the time available for repair. The survival data for normal human fibroblasts treated with N-AcO-AAF when the cells were growing at low density are also shown in Figure 1.9 (replotted from Figure 1.6). The slope of the exponential part of these survival data is nearly the same as the slope of the data for cells treated at confluence and immediately replated. However, the shoulder on the in-situ data is substantially smaller than that obtained when cells were treated at confluence. This suggests that the position of cells in the growth cycle may be an important consideration in modeling the shoulder on survival curves.

Estimates of the effect of recovery on the fraction of potentially lethal damage excised are given in Table 1.1. The fraction of damage excised is nearly independent of dose for a given recovery time. The slight tendency for the fraction to decrease with increasing dose is probably due to the shoulder on the survival response for normal cells treated at confluence. The fraction of damage excised at a dose of 5 μM when cells were immediately replated is used to estimate the time available for repair without recovery. This estimate is 142 h if the kinetics of excision are first order and 61 h if repair kinetics are processive. Given the time available for repair when cells are immediately replated, we predict the fraction of damage

Table 1.1. Effect of Recovery on the Fraction^(a) of AAF Residues Excised by Normal Human Fibroblasts

Dose, μM	f_0	f_{24}	f_{48}	f_{72}	f_{97}
2	0.90	0.99	0.96	0.95	0.98
3	0.86	0.92	0.94	0.97	0.98
4	0.88	0.92	0.94	0.95	0.97
5	0.88	0.92	0.94	0.95	0.97
first-order ^(b)	—	0.91	0.94	0.96	0.97
processive ^(c)	—	1.0	1.0	1.0	1.0

(a) $f_{\Delta} = 1 - \ln S_{\Delta} / \ln S_{XPA}$ where S_{Δ} is the survival of normal cells held in confluence for Δ hours between treatment and replating, and S_{XPA} is the survival of XP12BE cells.

(b) Model prediction assuming first-order excision kinetics.

(c) Model prediction assuming processive excision kinetics.

excised when the cells are held at confluence between treatment and replating. These results are shown in Table 1.1, where it can be seen that the increase in the extent of repair with recovery is predicted very well by our model when classical first-order kinetics are used. If the kinetics of excision repair are processive, the increase in time available for repair in the recovery experiments should be sufficient to remove all the damage. This is not observed in the experiments. The success of our model in explaining the effects of recovery on survival encourages us to investigate the mechanism of reproductive death in cells exposed to chemical carcinogens. This mechanism should be consistent with the time available for repair that is suggested by our analysis of the survival data.

Biological and Biochemical Experimentation with Coal-Related Carcinogens

C. N. Newman

In this project, active forms of polynuclear aromatic hydrocarbon pollutants generated during the utilization of coal are being studied so that their effects on mammalian cells can be modeled in tissue culture. The presumptive consequences of radiologically and chemically induced chromosome damage on cell survival, induced mutation, and repair processes are similar, and mathematical approaches to one type of damage have been applied to the other (Lawley 1979; Munson and Goodhead 1977). In general, both show a dose-dependent survival

and mutation response, and the damaged chromosomes appear to share common repair pathways (Maher and McCormick 1978).

Little information is available on the formation of carcinogen-induced damage at low concentrations of pollutants and on the corresponding significance of cellular repair processes other than error-free excision repair. Excision repair seems to predominate at high doses in human fibroblasts, but even so some lesions remain unexcised in viable cells (Maher and McCormick 1978). We do not know the consequences of residual damage, which may be cumulative at low doses. Because few if any lesions are excised from Chinese hamster ovary (CHO) cells, this cell system has been chosen to examine the fate of unexcised chemical lesions and to study other repair pathways that may be error-prone and may therefore bear more significantly on carcinogenesis.

Experiments in progress are designed to provide information on 1) the relationship between pollutant dose and cellular inactivation, mutation, and biochemical repair processes; 2) the kinetics of induction and repair of damage to deoxyribonucleic acid (DNA), and 3) the development of mutants with altered repair abilities. Repair-deficient CHO mutants have already been isolated (Stamato and Hohman 1975). We have approached this problem from a unique perspective by selecting repair-proficient mutants, cell lines with a repair ability more efficient than that of the parent cell line. For simplicity, we used ultraviolet (UV) light to induce lesions in cells because some of the enzymes that repair these lesions also repair some chemical-DNA adducts (Maher and McCormick 1978). Approximately 50 isolates have already been selected and are now being characterized with respect to enhanced repair abilities.

Figure 1.10 shows the survival of CHO cells after exposure to low concentrations of benzo[a]pyrene-4,5-epoxide. These data are consistent with the results obtained at higher doses by Huberman et al. (1976) using Chinese hamster V-79 cells. Even at low carcinogen concentrations, cellular inactivation is a simple exponential function, that is, there is no shouldered response. Figure 1.11 shows the corresponding alkaline CsCl density-gradient assay for replication repair of damaged DNA in cells treated with 0.8 μM of carcinogen. There is no detectable increase in the amount of ^3H -thymidine incorporated in parental DNA over a 45-h period, indicating

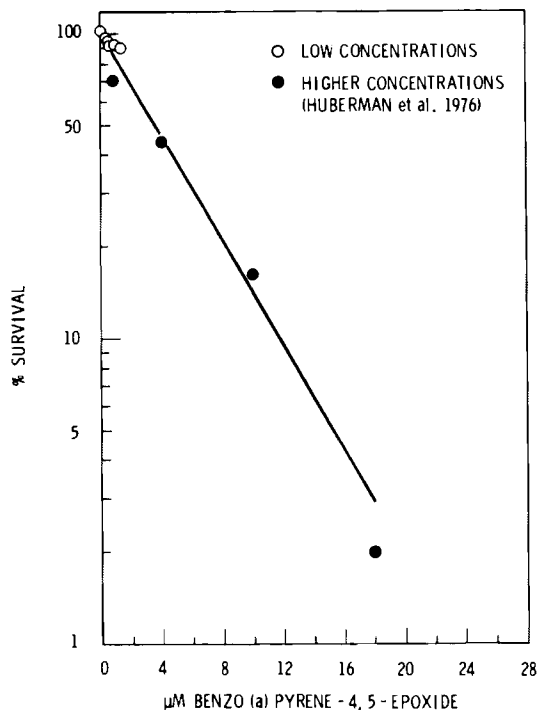


Figure 1.10. Survival of CHO Cells After Exposure to Benzo[a]pyrene-4,5-EpoXide

that little or no repair has occurred. Interestingly, preliminary data (not shown) failed to demonstrate the induction of mutants at doses up to 1.2 μM . This result contrasts with data shown in Figures 1.12 and 1.13 for cells treated with UV light. Low fluences of UV irradiation (<50 ergs/ mm^2) proved relatively inefficient at killing cells (in the shouldered region of the survival curve); however, the frequency of mutation induction appears to be a linear fluence-dependent function, extrapolating approximately through the origin. These findings are being examined further.

To study genetic damage in CHO cells treated with carcinogens, the hypoxanthine-guanine phosphoribosyl transferase (HGPRT) mutation system, as described by Hsie et al. (1975), was selected. The HGPRT enzyme is normally a component of a purine salvage pathway. When challenged with the purine analogue, 6-thioguanine (TG), wild-type cells with functional enzyme incorporate lethal quantities of this substance in their DNA while mutant cells, unable to synthesize HGPRT, survive. Expression of the mutant phenotype usually requires continuous growth and division for 7 to 9 days after treatment before cells can be

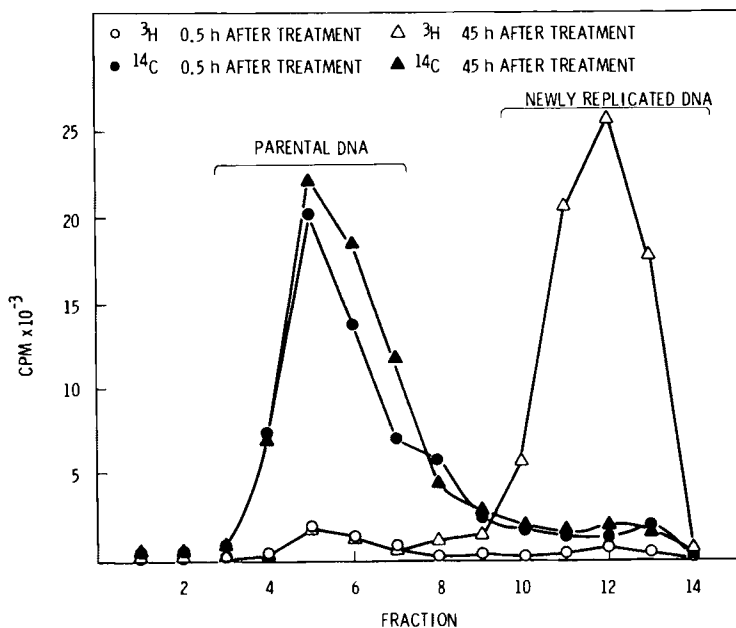


Figure 1.11. Replication Repair of CHO Cells Following Treatment with 0.8 μM of Benzo[a]pyrene-4,5-EpoXide. Cultures were grown for about five generations in medium containing ^{14}C -thymidine. After treatment with carcinogen, cells were grown in the presence of ^3H -TdR, BUdR, and FUDR and DNA was periodically analyzed on alkaline CsCl gradients.

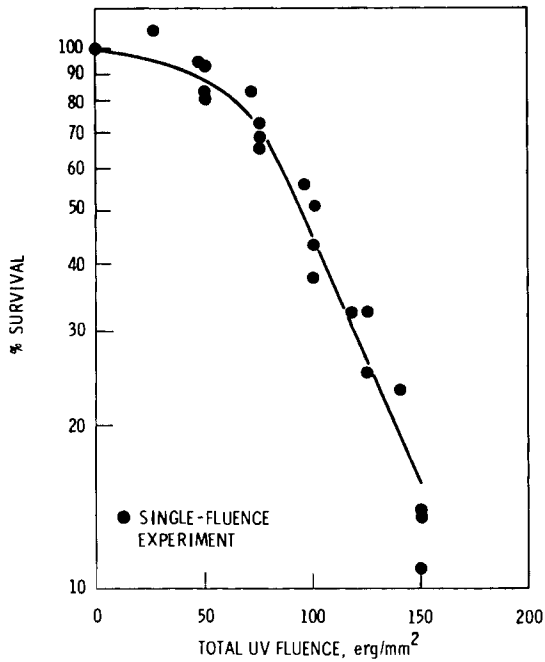


Figure 1.12. Inactivation of CHO Cells by Ultraviolet Light

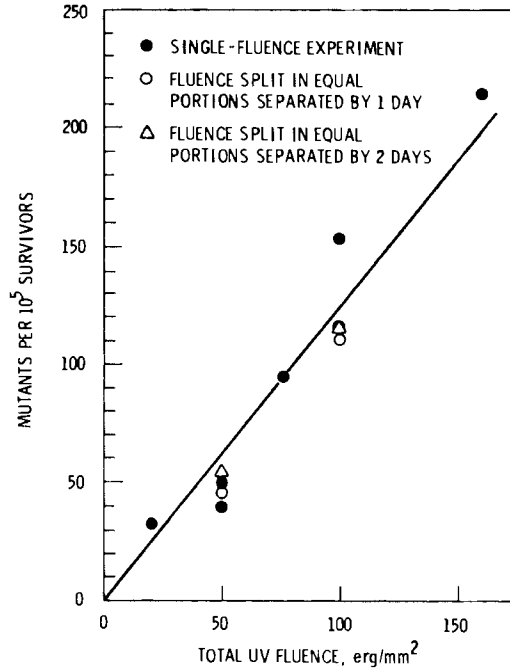


Figure 1.13. HGPRT Mutation Induction in CHO Cells by UV Light

challenged with TG. This expression period allows pre-existing HGPRT protein molecules to be diluted to low concentrations in mutant cells. Circumvention of the phenotypic expression period for HGPRT, one goal of this project, would greatly facilitate determination of the biological effect of residual damage, as will be discussed.

Figure 1.14 illustrates schematically the configuration of chemically-induced chromosomal lesions, C, in the HGPRT locus immediately after treatment ($G = 0$) and at up to two generations ($G = 2$) thereafter. Following the first round of semiconservative DNA replication and segregation of sister DNA molecules to daughter cells ($G = 1$), chemical adducts are confined to only one strand of a duplex. (Recombination is insignificant in CHO cells.) The fraction of cells with residual damage decreases by one half each generation, beginning at $G = 2$. If the damage remains biologically effective, then the number of

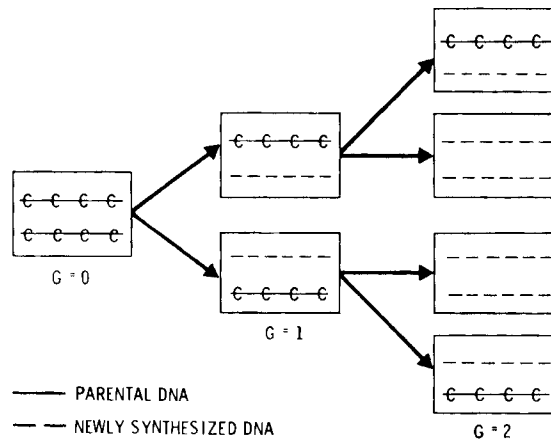


Figure 1.14. Schematic Representation of Carcinogen Residues, C, in HGPRT Locus of Cells at up to Two Generations, G, After Single Exposure to Chemical Carcinogen

HGPRT mutants per survivor after G generations of growth during the expression period is given by

$$M_G = p[C] + 1/2p[C] + \frac{1/2p[C]}{2} + \dots$$

$$+ \frac{1/2p[C]}{2^{G-1}}$$

here p is the probability per adduct of a mutation in the HGPRT locus and $[C]$ is the carcinogen dose. Each round of replication during the phenotypic expression period should increase the mutation frequency by 50% of the number of mutants formed in the previous generation. If damage on both strands is required for mutation of the HGPRT locus, then no enhancement of the mutation frequency caused by growth and division should be observed.

To determine the mutation yield after each generation, we are attempting to bypass the required 7 to 9 days of cell division prior to the challenge with TG, while still permitting phenotypic expression in nongrowing cells. The rationale for this effort is that natural protein turnover is enhanced in arrested cells (O'Neill and Hsie 1979); thus, if growth could be arrested immediately or at specific times after treatment, HGPRT would decay to low concentrations in nondividing mutant cells, probably over a 7- to 10-day period.

We have tried several methods for arresting cell growth. 1) Cells were kept in a serum-free medium in agar-coated flasks (to prevent attachment). The survival of these cells was variable from experiment to experiment and among cells from different culture vessels in the same experiment, ranging from 100% to 2% of the survival of untreated cells. 2) Cells were allowed to attach in growth medium diluted to 1% fetal calf serum (FCS). The results of a typical experiment of this type are shown in Figures 1.15 and 1.16. Cells in 1% FCS stopped growing at 3×10^4 cells/cm², while fully supplemented cells (10% FCS) grew to a density five to six times higher (Figure 1.15). Figure 1.16 shows the results of labeling these cells with 15-min pulses of ³H-thymidine to measure rates of DNA replication at various times after the medium shift. The rate of replication in serum-limited cells decreased continuously after 20 h to about 1% of the maximum rate in the control culture. Replication in the controls also declined after about 80 h when these cells entered the plateau phase. However, cells

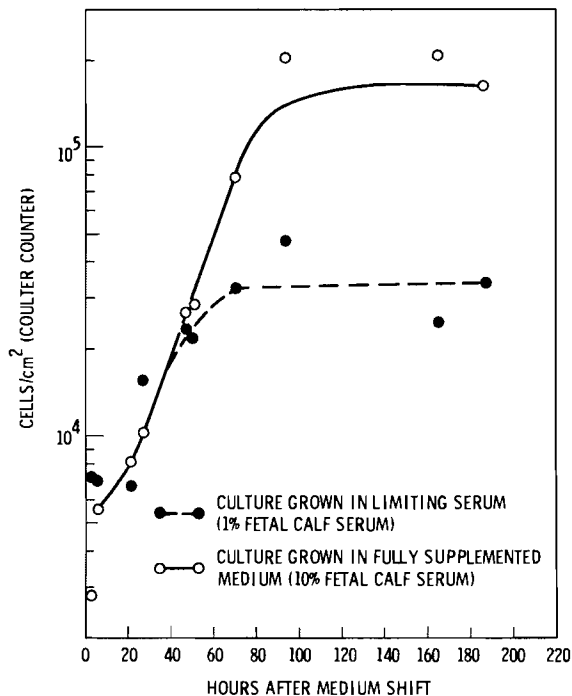


Figure 1.15. Inhibition of Cellular Growth by Serum Limitation

in the diluted medium remained viable (20% cloning efficiency), whereas the control culture did not. Experiments to improve the cloning efficiency of limited cells are directed toward maintaining culture pH within the physiological range over an extended time. The arresting of suspension cultures of CHO cells in 1% FCS is also being investigated, as suggested by R. Heflich of the National Center for Toxicology Research.

Experiments to examine the potential hazard of damage accumulated in DNA through tolerance mechanisms are also under way. If damage is effective only when it occurs on both DNA strands, then lesions on a single DNA strand may sensitize daughter cells to further exposure to the carcinogen. This effect should be observable in split-dose experiments. Figure 1.17 illustrates the configuration of lesions in the HGPRT locus that might result from equal fractions of a dose D separated by one generation. In this case we would expect the increase in mutation frequency caused by dose fractionation to be 25% of the single-dose value. The enhancement of the mutation frequency decreases rapidly as the interval

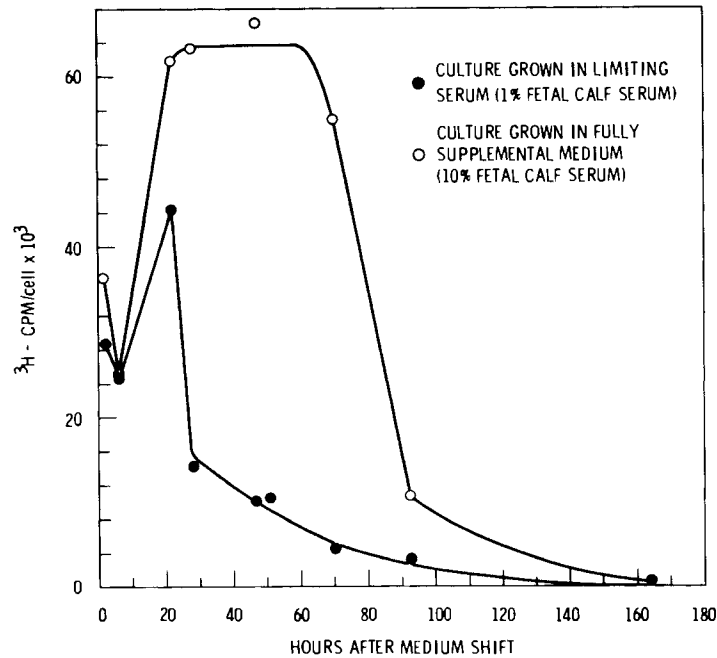


Figure 1.16. Rates of DNA Replication

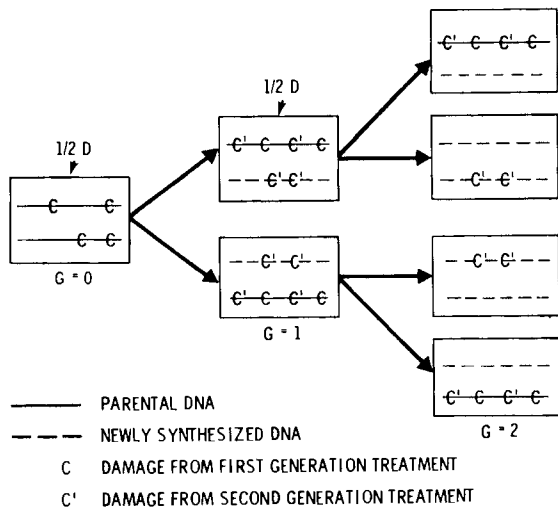


Figure 1.17. Schematic Representation of Carcinogen Residues in HGPRT Locus Resulting from Equal Fractions of a Dose, D, Separated by One Generation

between fractions increases because replication dilutes the population of cells that have been sensitized by the first fraction.

Figure 1.13 shows the results of a preliminary split-dose experiment using UV light as the carcinogen. Equal fluences were given 1 or 2 days apart (approximately 2 and 4 generations, respectively), followed by 8 days of growth for expression of HGPRT mutants. No significant increase in the mutation frequency was observed for the split-dose treatment relative to the single-dose treatment. The time interval between treatments may have been too large to give an enhancement greater than the usual statistical fluctuations. Control of DNA replication through growth arrest should increase the sensitivity of these split-dose experiments.

Permeabilities of Model Lung-Cell Membranes to Coal Pollutants

D. R. Kalkwarf

Sulfur dioxide and polycyclic aromatic hydrocarbons are pollutants common to stack emissions from all coal-fired power plants. Sulfur dioxide and its hydrolysis products, HSO_3^- and SO_3^{2-} , are known to be lung irritants; recent reports (Hayatsu 1976; Shapiro 1977) suggest that they could also exert mutagenic effects on lung cells. The probability of this occurring would depend

on the ability of the dominant species at physiological pH, HSO_3^- , to cross the cytoplasmic and nuclear membranes and react with deoxyribonucleic acid (DNA) before being oxidized to the relatively innocuous SO_4^{2-} . Similarly, some polycyclic aromatic hydrocarbons (PAHs) such as benzo[a]pyrene have been shown to be carcinogenic in skin-painting tests on mice, but the kinetics of PAH uptake by lung cells is not known in sufficient detail to predict rates of PAH diffusion into the cell nucleus or even to predict whether PAHs can diffuse across cell membranes at significant rates without chemical alteration of the PAH to a more polar derivative.

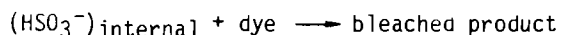
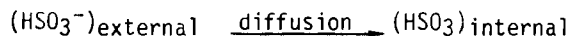
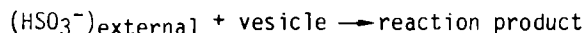
To estimate how rapidly HSO_3^- and representative PAHs diffuse across lung-cell membranes, we have evaluated the permeability coefficients of lung-phospholipid bilayer membranes to these pollutants in vitro. The results obtained to date indicate that HSO_3^- diffuses across these basic structural barriers in lung cells with its chemical reactivity intact as rapidly as Cl^- , but that the PAH, pyrene, does not enter these bilayers in unmodified form.

The phospholipid membranes were prepared in the form of residues by sonicating 2% suspensions of either dipalmitoylphosphatidylcholine or stearoyl sphingomyelin in $\mu = 0.20$ sodium phosphate buffer at pH 6.0. Multilayered residues were removed by centrifugation and the remaining vesicles, each bounded by a single phospholipid bilayer, were used in this investigation.

These structures have an outer diameter of 25 nm and a membrane thickness of 6 nm, and are shown schematically in Figure 1.18.

Permeability evaluations for HSO_3^- were based on the bleaching rates of dye-loaded vesicles exposed to external HSO_3^- . Basic Violet 15 (C.I. 42510), a dye that is selectively bleached by HSO_3^- , was used for this purpose. Solutions of this dye in the above-mentioned buffer were incorporated inside the vesicles during sonication, and exterior dye solution was removed by passing the vesicle suspension through a Sephadex G-75 gel-filtration column. The absorbance of the dye-loaded vesicle suspension was then monitored at 539 nm with a spectrophotometer before and after the addition of a measured amount of HSO_3^- solution. Independent measurements showed negligible leakage of dye from the vesicles during this period. In suspensions where the vesicles contained no dye but were surrounded by dye, the bleaching rates were found to be much greater initially, as shown in Figure 1.19.

Permeability coefficients were calculated on the basis of the following mechanism:



Assuming that the reactions of HSO_3^- with dye or vesicles are all kinetically second

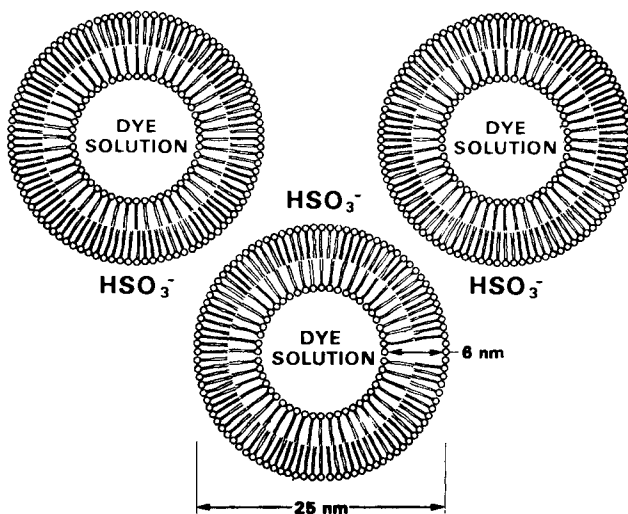


Figure 1.18. Cross Sectional View of Dye-Loaded Vesicles Exposed to External HSO_3^-

order, this mechanism predicts that the permeability coefficient, P , is given by

$$P = \left(\frac{V_i}{at} \right) \frac{(dA/dt)_{\text{dye inside}}}{(dA/dt)_{\text{dye outside}}}$$

for small values of time t , where A is the absorbance of the vesicle suspension at 539 nm and V_i/a is the ratio of the in-

ternal volume of a vesicle to its internal surface area, 2.2×10^{-7} cm.

Values obtained in this study are compared with those for other systems in Table 1.2. The assumed mechanism was considered to be verified by the constancy of P over a hundred-fold range of HSO_3^- concentration. These results demonstrate

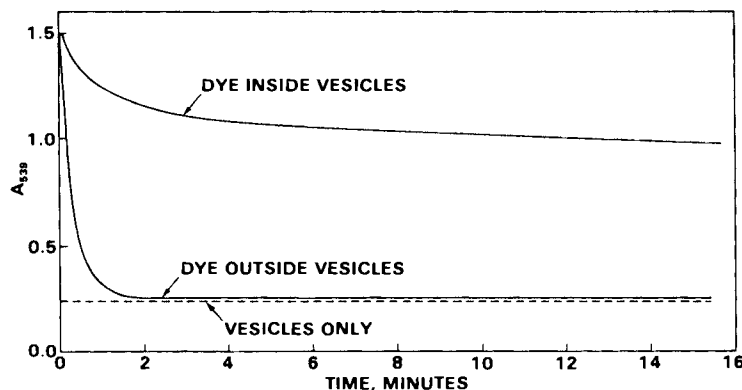


Figure 1.19. Bleaching of Dye-Loaded Vesicle Suspensions by Addition of External HSO_3^-

Table 1.2. Permeability Coefficients of Anions Through Phospholipid Bilayers

Bilayer and Temperature	Permeability Coefficient, cm/s	[HSO_3^-], M pH	
Dipalmitoylphosphatidylcholine, 23°C(b)	$P_{\text{HSO}_3^-} = 1.8\text{E-}9$ (a)	4E-2	6.0
	1.9E-9	4E-3	6.0
	1.8E-9	4E-4	6.0
Stearoyl sphingomyelin, 23°C(b)	$P_{\text{HSO}_3^-} = 3.9\text{E-}9$	1E-3	4.2
	4.6E-9	1E-4	6.0
	4.3E-9	1E-5	6.0
Egg phosphatidylcholine, 20°C	$P_{\text{maleate}} = 4\text{E-}9$ (c)		
	$P_{\text{chloride}} = 1.1\text{E-}10$ (d)		
Egg phosphatidylcholine/n-tetradecane, 20°C(e)	$P_{\text{chloride}} = 2.4\text{E-}7$		
Diphytanoylphosphatidylcholine/n-decane, 20°C(d)	$P_{\text{chloride}} = 6.8\text{E-}8$		

(a) $1.8\text{E-}9 = 1.8 \times 10^{-9}$

(b) Reference: This work

(c) Reference: Prestegard, Cramer and Viscio 1979

(d) Reference: Toyoshima and Thompson 1975

(e) Reference: Pagano and Thompson 1968

that HSO_3^- can cross the basic phospholipid bilayer structure in cell membranes about as fast as chloride ion. Since no extrinsic carriers or membrane pore-formers are present to facilitate this movement, it is estimated that cell membranes would be at least as permeable to HSO_3^- ions, and these species should be available for reaction with cellular DNA.

Permeability evaluations for pyrene were based on expected changes in the fluorescence intensity from vesicles whose interiors were filled with 0.1 M caffeine in aqueous solution and whose exteriors were suddenly exposed to solutions of pyrene in water. The solubility of pyrene was found to increase from 5×10^{-6} in water to 2×10^{-3} M in aqueous 0.1 M caffeine, and this solubility difference should act as a

driving force for pyrene diffusion across the bilayer. On exposure of the vesicle exteriors to pyrene, their fluorescence emission was expected to rise as the pyrene diffused from a medium of high dielectric constant, the bilayer, and then to decrease as the pyrene diffused from the bilayer into the aqueous interior. Instead, the intensity of the 380-nm fluorescence from pyrene remained constant, indicating that no pyrene diffusion was occurring.

A similar constancy in 380-nm fluorescence intensity was observed when pyrene-saturated water was added to CHO cells suspended in nutrient solution. These results suggest that PAHs cannot enter phospholipid bilayers without being chemically altered to more polar derivatives.

REFERENCES

- Hayatsu, H. 1976. "Bisulfite Modification of Nucleic Acids and Their Constituents." In Progress in Nucleic Acid Research and Molecular Biology, ed. W. Cohn, Vol. 16, pp. 75-124. Academic Press, New York.
- Haynes, Robert H. 1975. "The Influence of Repair Processes on Radiobiological Survival Curves." In Cell Survival After Low Doses of Radiation: Theoretical and Clinical Implication, pp. 197-208. The Institute of Physics and John Wiley & Sons, London.
- Heflich, R. H., R. M. Hazard, L. Lommel, L. D. Scribner, V. M. Maher and J. J. McCormick. 1980. "A Comparison of the DNA Binding, Cytotoxicity and Repair Synthesis Induced in Human Fibroblasts by Reactive Derivatives of Aromatic Amide Carcinogens." Chemical-Biological Interactions 29:43-56.
- Hsie, A. W., P. A. Brimer, T. J. Mitchell and D. G. Gosslee. 1975. "A Dose-Response Relationship for Ultraviolet-Light-Induced Mutations at the Hypoxanthine-Guanine Phosphoribosyltransferase Locus in Chinese Hamster Cells." Som. Cell Genet. 1:383-389.
- Huberman, E., L. Sachs, S. K. Yang and H. U. Gelboin. 1976. "Identification of Mutagenic Metabolites of Benzo(a)pyrene in Mammalian Cells." Proc. Nat. Acad. Sci. 73:607-611.
- Lawley, P. D. 1979. "Approaches to Chemical Dosimetry in Mutagenesis and Carcinogenesis: Relevance of Reactions of Chemical Mutagens with DNA." In Chemical Carcinogens and DNA, ed. P. L. Grover, Vol. I, pp. 1-36. CRC Press, Inc., Boca Raton, Florida.
- Levinson, J. W., B. Konze-Thomas, V. M. Maher and J. J. McCormick. 1979. "Evidence for a Common Rate Limiting Step in the Repair Process of Ultraviolet Light (UV) and N-Acetoxyacetamino Fluorene (N-AcO-AAF) Induced Damage in the DNA of Human Fibroblasts." Proceedings of the 17th Annual Meeting of the American Association for Cancer Research, New Orleans, May 16-19, 1979, p. 105.
- Maher, V. M., N. Birch, J. R. Otto and J. J. McCormick. 1975. "Cytotoxicity of Carcinogenic Aromatic Amides in Normal and Xeroderma Pigmentosum Fibroblasts with Different DNA Repair Capabilities." Journal of the National Cancer Institute 54:1287-1293.
- Maher, V. M., and J. J. McCormick. 1978. "Mammalian Cell Mutagenesis by Polycyclic Aromatic Hydrocarbons and Their Derivatives." In Polycyclic Hydrocarbons and Cancer, Vol. 2, pp. 137-160. Academic Press, New York.
- McCann, J., and B. N. Ames. 1976. "Detection of Carcinogens as Mutagens in the Salmonella/Microsome Test: Assay of 300 Chemicals: Discussion." Proc. Nat. Acad. Sci. 73:950-954.
- Munson, R. J., and D. T. Goodhead. 1977. "The Relation Between Induced Mutation Frequency and Cell Survival--A Theoretical Approach and an Examination of Experimental Data for Eukaryotes." Mut. Res. 42:145-159.
- O'Neill, J. P., and A. W. Hsie. 1979. "Phenotypic Expression Time of Mutagen-Induced 6-Thyoguanine Resistance in Chinese Hamster Ovary Cells." Mut. Res. 59:109-118.
- Pagano, R., and T. E. Thompson. 1968. "Spherical Lipid Bilayer Membranes: Electrical and Isotopic Studies of Ion Permeability." J. Mol. Biol. 38:41-52.
- Prestegard, J. H., J. A. Cramer and D. B. Viscio. 1979. "Nuclear Magnetic Resonance Determinations of Permeation Coefficients for Maleic Acid in Phospholipid Vesicles." Biophys. J. 26:575-584.
- Shapiro, R. 1977. "Genetic Effects of Bisulfite (Sulfur Dioxide)." Mut. Res. 39:159-176.
- R. D. Smith. 1979a. "A Direct Mass Spectrometric Study of the Mechanism of Toluene Pyrolysis at High Temperatures." J. Phys. Chem., 83:1553.
- R. D. Smith. 1979b. "Formation of Radicals and Complex Organic Compounds by High-Temperature Pyrolysis: The Pyrolysis of Toluene." Combust. Flame, 35:179-190.
- Stamato, T. D., and L. K. Hohman. 1975. "A Method for Replica Plating CHO Cells using Nylon Cloth." Cytogenet. Cell Genet. 15:372-379.
- Toyoshima, Y., and T. E. Thompson. 1975. "Chloride Flux in Bilayer Membranes: Chloride Permeability in Aqueous Dispersions of Single-Walled Bilayer Vesicles." Biochem. 14:1525-1531.